Akita J Med **39** : 129–137, 2012

PHOSPHATIDYLINOSITOL 3,5–BISPHOSPHATE IS AN ESSENTIAL REGULATOR OF LYSOSOME MORPHOLOGY

Ken Asanuma, Shunsuke Takasuga, Junko Sasaki and Takehiko Sasaki

(received 17 January 2013, accepted 23 January 2013)

Department of Medical Biology, Akita University Graduate School of Medicine, Akita 010–8543, Japan

Abstract

Phosphoinositides are lipid second messengers that act as key players in endosomal membrane trafficking, and mutations in several phosphatases that metabolize these lipids cause severe genetic diseases. We previously reported that type III phosphatidylinositol phosphate kinase (PIPKIII) is a critical regulator of lysosome size. However, the lipid products that mediate PIPKIII function have not been well characterized. Using a series of phosphoinositide phosphatase expression vectors, we show here that phosphatidylinositol 3,5–bisphosphate is the obligatory lipid for lysosome morphology.

Key words : MTMR14, PIPKIII, phosphatidylinositol 3,5–bisphosphate, lysosome

Introduction

Lysosomes are cytoplasmic organelles delimited by a lipid monolayer and contain a variety of hydrolytic enzymes that degrade the vast majority of cellular molecules entering lysosomes via endocytosis, phagocytosis, or autophagy. In light of the growing number of physiological functions, associations between lysosome malfunction and human pathologies have also been strengthened. For instance, lysosomal dysfunction is associated with cancer, neurodegeneration, heart failure, microbial infection and aging[1–5]. These conditions can stem from deficiencies in lysosomal hydrolases as evidenced by human hereditary diseases, but also from altered phospholipid metabolism that perturbs intracellular membrane trafficking and leads to abnormal size and function of the organelle[6–8].

Phosphoinositides are molecules that contain phosphatidylinositol (PI), a major class of membrane phospholipid, with a glycerol backbone, two long–chain fatty acids linked to the glycerol through ester bonds, and an inositol head group linked to the glycerol through a phosphate group. When the hydroxyl residues at the 3, 4, and 5 positions of the inositol ring are phosphorylated in varying combinations, 7 different phosphoinositide species can be generated[9]. In mammals, 18 interconversion reactions involving all 8 phosphoinositide species have been identified. These reactions are mediated by 48 genes encoding 19 phosphoinositide kinases and 29 phosphoinositide phosphatases[9]. Among the phosphoinositide metabolizing enzymes, type III phosphatidylinositol phosphate kinase (PIPKIII) has been implicated in control of the size and function of lysosomes. Inactivation of PIPKIII in both mammalian cells and yeast cells, resulted in the formation of enlarged cytoplasmic vacuoles of lysosomal origin[10]. Recently, we reported that PIPKIII–null mouse embryos died by embryonic day 8.5 due to failure of the visceral endoderm to supply the epiblast with maternal nutrients as a consequence of lysosomal vacuolation[8]. Similarly, intestinal–specific PIPKIII–deficient mice failed to thrive and eventually died of malnutrition due to defective membrane trafficking in the mu-

Correspondence : Takehiko Sasaki, Ph. D.
Department of Medical Biology Akita University Graduate School of Medicine, 1–1–1 Hondo, Akita 010–8543, Japan
Tel : 018–884–6080
Fax : 018–836–2607
E–mail : tsasaki@med.akita–u.ac.jp

tant enterocytes with swollen lysosomes[8]. Although these findings have identified a critical role of PIPKIII in the physiological control of lysosomal functions, the relationship between phosphoinositide metabolism and disorders of lysosome is still not understood.

PIPKIII phosphorylates PI and PI-3-monophosphate (PI3P) *in vitro* to produce PI-5-monophosphate (PI5P) and PI-3,5-bisphosphate [PI(3,5)P_2], respectively[11]. Conversely, there are several phosphatases that dephosphorylate the substrates and the products of PIPKIII[9]. For instance, myotubularin (MTM) and myotubularin-related proteins (MTMRs) which constitute a large family of phosphatases, dephosphorylate those phosphoinositides[12-14]. Functions of MTM and MTMRs are poorly understood.

To gain insight into the obligate lipid regulating lysosomal homeostasis, we screened phosphoinositide phosphatases for their effects on lysosomal morphology. Our results demonstrate that PI(3,5)P_2, and not PI3P or PI5P, is a responsible phosphoinositide for controlling lysosomal morphology.

Materials and methods

Expression vectors for phosphoinositide phosphatases

MTM1, MTMR3, MTMR4, MTMR8, MTMR14, INPP5B, OCRL1, PIPP, SKIP, Pharbin, and PLIP cDNAs were obtained by reverse transcription-PCR. MTMR1, MTMR2, MTMR6, MTMR7, Tmem55a, Tmem55b, and SYNJ2 cDNAs were obtained from Invitrogen. SAC1, SAC2 and SYNJ1 cDNAs were obtained from the Kazusa DNA Research Institute. PTEN cDNA was kindly given by Dr. A. Suzuki (Kyusyu University). SAC3 cDNA was provided by Dr. T. Takenawa (Kobe University). SHIP1 and SHIP2 cDNAs were given by Dr. C. Erneux (IRIB-

Table 1. PCR primer pairs to create the restriction enzyme sites on the 5′ and 3′ ends of the open reading frame.

	Sense Primer	Antisense Primer
MTM1	5′-GCGAGATCTGCTTCTGCATCAGCATCTAAG-3′	5′-GCGGATCCAAGTGCAGTGCCAGAAGTGAG-3′
MTMR1	5′-GCGGATCCGACAGGCCAGTGGCGGCGGCGG-3′	5′-GCGTCTAGATCAGACTGAGGTGTGTACAGG-3′
MTMR2	5′-GCGGTACCGAGACGAGCTCGAGCTGCGAGA-3′	5′-GCGGGCCCTTATACAACAGTTTGGACAGGA-3′
MTMR3	5′-GCGGATCCGATGAAGAGATGCGGCATAGCC-3′	5′-GCGTCTAGATCAGTTTGAAGTGGCAGCAAT-3′
MTMR4	5′-GCAAGCTTGGTGAGGAGGGCCCCCCCAGCC-3′	5′-GCCTCGAGTCAACTGGAAGCCGTAGCAATG-3′
MTMR6	5′-GCGGATCCGAGCACATCCGGACAACCAAGG-3′	5′-GCGTCTAGACTAACAAGTCATTCTGGCCAC-3′
MTMR7	5′-GCGGATCCGAGCACATCCGCACGCCCAAGG-3′	5′-GCGTCTAGATTAGGCAGTGAGAAACACAGC-3′
MTMR8	5′-GCGGATCCGATCATATTACGGTACCCAAGG-3′	5′-GCCTCGAGTCACTGATGCTTGGAGTAGTCT-3′
MTMR14	5′-GCAAGCTTGCGGGTGCTCGGGCCGCCGCCG-3′	5′-GCGGGCCCTCACAAGGTGCTGGTGCTTGTG-3′
PTEN	5′-GGATCCGACATGACAGCCATCATCAAAGAGA-3′	5′-CTCGAGTCAGACTTTTGTAATTTGTGAATG-3′
Tmem55a	5′-GCAAGCTTGCTGCTGACGGGGTGGACGAAC-3′	5′-GCGGATCCTTAAGCAAAGCCGTGCTCTGGA-3′
Tmem55b	5′-GCGGATCCGCGGCAGACGGAGAGCGCTCCC-3′	5′-GCCTCGAGTCAGGAGAAGTTCTGGACAGGA-3′
SAC1	5′-GCGGATCCGCGGCCGCAGCCTACGAGCATC-3′	5′-GCGGTCGACGCCGCTTTCCACAAACACAAA-3′
SAC2	5′-GCGGATCCGAGCTCTTTCAGGCTAAGGACC-3′	5′-GCGGCGGCCGCAAAGGAATGTGACTAAAAT-3′
SAC3	5′-CCAAGCTTATGCCCACGGCCGCCG-3′	5′-CCCTCGAGTCACAGGTAGCGGTTCCTGATGTACTCTC-3′
INPP5B	5′-GCGCGGCCGCGACCAGTCTGTGGCAATCCA-3′	5′-GCGCGGCCGCCAGGAGAGGAGTAGTGAGGC-3′
OCRL1	5′-GCGGATCCGAGCCGCGGCTCCCGATTGGAG-3′	5′-GCGCTCGAGGAATCTCGGATAGGAAAAGAC-3′
PIPP	5′-GCGGCCGCGAAGGCCAGACCAGGAGTGGTA-3′	5′-GCTCTAGATCAGGGCCCCAAACCCCCTTCC-3′
SYNJ1	5′-GCGGTACCGCGTTCAGCAAAGGATTTCGAA-3′	5′-GCCTCGAGTTATCTTTCCGTGAAGTCCAAT-3′
SYNJ2	5′-GCGGATCCTCAGTGGGCAGAATTCCAGATG-3′	5′-GCGCGGCCGCGTCACCTTCATGCCTGTGGG-3′
SKIP	5′-GCGGATCCCAGCACGGAGACAGGAACACAC-3′	5′-GCGCTCGAGTTCATTCACTTCCATCTGGGC-3′
SHIP1	5′-GCGAAGCTTGTCCCCTGCTGGAACCATGGC-3′	5′-GCGGGATCCAGTGGCAGCTCACTGAGGGCT-3′
SHIP2	5′-GCGAAGCTTGCCCCCTCCTGGTACCACCGC-3′	5′-GCGCTCGAGAGCTTCGTGGTGCCTCCGCTA-3′
Pharbin	5′-GCGGATCCCCATCCAAGTCAGCTTGCCTGC-3′	5′-GCGCTCGAGGCCAGTCCTGGTCTGGAATCT-3′
PLIP	5′-GCGGATCCGCAGCATCCGCGTGGCTGGAGG-3′	5′-GCGCTCGAGTTAATTCTTTGCTGCCCTTGC-3′

Table 2. Mutated PCR primer pairs to construct phosphatase-defective mutants (PD).

	Sense Primer	Antisense Primer
MTM1 PD	5′-GTGCACTCCAGTGACGGATGGGACAGGACCGC-3′	5′-GTCACTGGAGTGCACAAGTACCGAGCTCTTTCC-3′
MTMR1 PD	5′-ATCCACTCGAGTGATGGGTGGGATCGAACATCC-3′	5′-ATCACTCGAGTGGATGACCACGGAAGTTTTCCC-3′
MTMR2 PD	5′-GTGCACTCGAGTGATGGTTGGGATCGCACAGCT-3′	5′-ATCACTCGAGTGCACTACCACAGACGTCTTCCC-3′
MTMR3 PD	5′-GTGCACTCGACCGATGGCTGGGATCGGACTCCC-3′	5′-ATCGCTCGAGTGCACTAGCACTGGTCGCTGATC-3′
MTMR4 PD	5′-GTACACTCGAGTGACGGCTGGGACCGTACACCA-3′	5′-GTCACTCGAGTGTACCAGCACAGGCCGGCCTTC-3′
MTMR6 PD	5′-GTCCACTCGAGCGATGGGTGGGACAGGACCTCC-3′	5′-ATCGCTCGAGTGGACCAACACACTTGCATTTTC-3′
MTMR7 PD	5′-GTTCACTCTTCTGACGGCTGGGACAGAACGGCC-3′	5′-GTCAGAAGAGTGAACAAGCACACTTGCCCCTTC-3′
MTMR8 PD	5′-GTCCACTCGAGTGATGGATGGGACCGCACAGCA-3′	5′-ATCACTCGAGTGGACTAAGACACTGGCCTTTTC-3′
MTMR14 PD	5′-CTGGTGCACTCTATCTCAGGCTGGGACCGGACC-3′	5′-GATAGAGTGCACCAGCAGCCCGCTGTCATCATC-3′
PTEN PD	5′-ATTCACTGGAAGGCTGGAAAGGGACGGACTGGT-3′	5′-AGCCTTGGAGTGAATTGCTGCAACATGATTGTC-3′
Tmem55a PD	5′-CTACTGATATCTAAGGATACATCTCGGCGAATA-3′	5′-CTTAGATATCAGTAGACAATTACAAGGGCATCT-3′
Tmem55b PD	5′-CTCCTGATATCCAAAGTGACTTCTCAGCGGATT-3′	5′-TTTGGATATCAGGAGACAATTACAGGGGCATCG-3′
SAC1 PD	5′-TTCAGATCTAACTCCATGGATTGTCTAGACAGA-3′	5′-GGAGTTAGATCTGAAAACTCCGTCCTGGTTTGT-3′
SAC2 PD	5′-CGAGTGAATTCCATGGACTGCCTGGATCGCACC-3′	5′-CATGGAATTCACTCGAAAAATCCCTTCTTGCTT-3′
SAC3 PD	5′-GTTTAGATCGCACCAACACAGCACAGTTTATG-3′	5′-CGATCTAAACAGTCCACAGAGTTGGTTCGAAGG-3′
INPP5B PD	5′-TGTGCTCGAATTCTGTGGAAAGGAAAGAACATC-3′	5′-CAGAATTCGAGCACACCAGGCCGGTGCACGACA-3′
OCRL1 PD	5′-TGTGCACGGATCCTTTGGAGAGGAATAAATGTT-3′	5′-AAGGATCCGTGCACACCAGGCGGGAACTCGGCA-3′
PIPP PD	5′-TGGACAGCTCGGATTCTGTGGAAGGTCAAGGCT-3′	5′-AATCCGAGCTGTCCAGGCTGGCTTCCGCTTTTT-3′
SYNJ1 PD	5′-TGGACAGCACGTGTCCTCTGGAGAAGGAGGAAG-3′	5′-GACACGTGCTGTCCAAGCAGGGGTGCGACACTT-3′
SYNJ2 PD	5′-TGGACAGCTCGAGTGCTGTGGTGGAGGAAGAAG-3′	5′-CACTCGAGCTGTCCAGGCTGGGGTACGGCACTT-3′
SKIP PD	5′-TGGACTGCCCGGATCCTGTGGAGGTTGAAGCGG-3′	5′-GATCCGGGCAGTCCACGCAGGCTTGCGTTTTTT-3′
SHIP1 PD	5′-TGGTGTGCTCGAGTCCTCTGGAAGTCTTATCCC-3′	5′-GACTCGAGCACACCAGGAAGGCAAGTTGTACTT-3′
SHIP2 PD	5′-TGGTGTGCACGGATTCTGTGGAAATCCTACCCT-3′	5′-AATCCGTGCACACCATGAGGGCACATTGGTCCG-3′
Pharbin PD	5′-TACACAGCTCGAGTCCTATACAAAAGCCGTCAC-3′	5′-GAGTCGAGCTGTGTAGGAGGGTGTCCTTTGCTT-3′
PLIP PD	5′-GCGGATCCGCAGCATCCGCGTGGCTGGAGG-3′	5′-GCGCTCGAGTTAATTCTTTGCTGCCCTTGC-3′

HM).

The cDNAs were subcloned into the pGEM-T Easy vector (Promega). After sequences were verified, restriction enzyme sites on the 5′ and 3′ ends of the open reading frame were created by PCR, and cDNAs were then subcloned into the pcDNA3.1 Hygro (+) N-FLAG vector (Invitrogen). Primer pairs used were shown in Table 1.

To construct phosphatase-defective mutants (PD), site-directed mutagenesis was carried out by PCR using mutated primers. Primer pairs used were shown in Table 2.

FLAG-tagged INPP4A wild-type (WT) and PD expression vectors were kindly provided by Dr. L. Stephens (Babraham Institute). FLAG-tagged INPP4B WT and PD expression vectors were given by Dr. T. Maehama (National Institute of Infectious Diseases).

Expression vectors for LAMP1 and IpgD

LAMP1 cDNA was obtained by reverse transcription-PCR, and then subcloned into pEGFP-N3 vector (Clontech) (sense primer, 5′-CCGAATTCGCCTCTCGAGTCGGTGGACG-3′, antisense primer, 5′-CCGGATCCGATGGTCTGATAGCCGGCGTG-3′). GFP-tagged IpgD WT and PD expression vectors were kindly provided by Dr. B. Payrastre (INSERM).

Transfection and Western blotting

One day prior to transfection, 4×10^5 HeLa cells (RIKEN) per well were plated in 2 mL of Dulbecco's MEM (Wako) supplemented with 10% FCS (GIBCO) and 0.1 mM non-essential amino acids (GIBCO) in 6-well plates. The cells were transfected with FLAG-tagged phosphatase expression vector using Lipofectamine™ 2000 transfection reagent (Invitrogen) according to the manu-

facturer's instructions. After transfection, cells were cultured for 24 h at 37°C in a 5% CO_2 incubator. Cells were washed twice with PBS and scraped into 100 μL of lysis buffer (20 mM Tris-HCl, 150 mM NaCl, 0.5% Triton X-100). To verify the phosphatase protein overexpression, 40 μg of cell lysates were separated by SDS-PAGE, blotted onto a PVDF membrane, and developed using an anti-FLAG M2 monoclonal antibody (Sigma) and a sheep anti-mouse IgG horseradish peroxidase-linked $F(ab)_2$ (GE Healthcare).

Morphological analysis

MTMR14 WT or PD expression vectors were co-transfected with GFP-LAMP1 expression vectors into HeLa cells. After transfection, the cells were cultured for 24 h at 37°C in a 5% CO_2 incubator. Cells were washed twice with PBS and trypsinized. The cells were then re-seeded in 35 mm glass-bottom dishes (MATSUNAMI) at a density of 4×10^4 cells/dish. The live cell imaging and morphological analysis were performed using an automated microscope system (DMI6000B. Leica).

GFP-IpgD WT or PD expression vectors were transfected into HeLa cells alone or together with MTMR14 WT. After transfection, the cells were treated and imaged as described above.

Quantitative analysis of enlarged lysosomes

HeLa cells were transfected with GFP-IpgD WT or PD expression vectors as described above. After transfection, the cells were cultured for 24 h at 37°C in a 5% CO_2 incubator, washed twice with PBS, and trypsinized. The cells were then re-seeded onto 35 mm glass-bottom dishes and cultured for 24 h. The cells were incubated with or without 2.5 μM PIPKIII inhibitor YM201636 (Calbiochem) for 4 h at 37°C in a 5% CO_2 incubator, and imaged as described above. Among the GFP-positive cells, the numbers of cells with enlarged vacuoles were quantified.

Measurements of phosphoinositides

HeLa cells were transfected with MTMR14 WT or PD expression vectors as described above. Cells were cultured in transfection medium for 4 h and then in orthophosphate-free DMEM (GIBCO) containing 1 mCi of [^{32}P]-orthophosphate (Perkin Elmer) for 24 h at 37°C in a 5% CO_2 incubator. Cells were washed twice with PBS and scraped in 800 μL 2% $HClO_4$. Resulting extracts were mixed with 3 mL of chloroform/methanol (1 : 2) and vortexed. The mixture were then incubated at room temperature for 10 min, and mixed with 1 mL each of $CHCl_3$ and 2% $HClO_4$ to separate the organic phase and aqueous phase. After centrifugation, the lower organic phase was recovered and mixed with 1 mL of $CHCl_3$-saturated 0.5% NaCl/1% $HClO_4$. The mixtures were vortexed well and then centrifuged. After centrifugation, the lower organic phase was recovered and dried in a SpeedVac. Dried lipids were deacylated with 1 mL of 40% methylamine : H_2O : methanol : n-butanol (24 : 16 : 40 : 10), incubated at 53°C for 1 h, dried in a SpeedVac, and resuspended in 800 μL of n-butanol : petroleum ether : ethyl formate (20 : 40 : 1) and 800 μL H_2O. After centrifugation, the aqueous phase was transferred and dried in a SpeedVac, and the resulting samples were resuspended in 130 μL of 10 mM $(NH_4)_2HPO_4$, pH 3.3, and separated by high performance liquid chromatography (HPLC) on a PartiSphere SAX column (Whatman). The column was developed with a gradient of 1 M $(NH4)_2HPO_4$, pH 3.3. The gradient began at 0% for 10 min, 0-20% for 96 min, 20-100% for 4 min, and remained at 100% for 10 min. The flow rate was 1.0 mL/min. The radioactivity was quantified with a Flow Scintillation Analyzer FSA610 (Perkin Elmer).

Statistical analysis

Data were presented as the mean±standard error of the mean (SEM), and were analyzed using Statcel2 software (OMS). Paired data were compared by two-tailed Student's *t* test. Comparisons between multiple groups were analyzed by analysis of variance (ANOVA) followed by Bonferroni's *post-hoc* test. Results with $P<0.05$ were considered statistically significant.

Results and Discussion

We constructed a set of vectors expressing 27 phosphoinositide phosphatases and phosphatase-inactive mutants of each enzyme. Successful FLAG expressions of

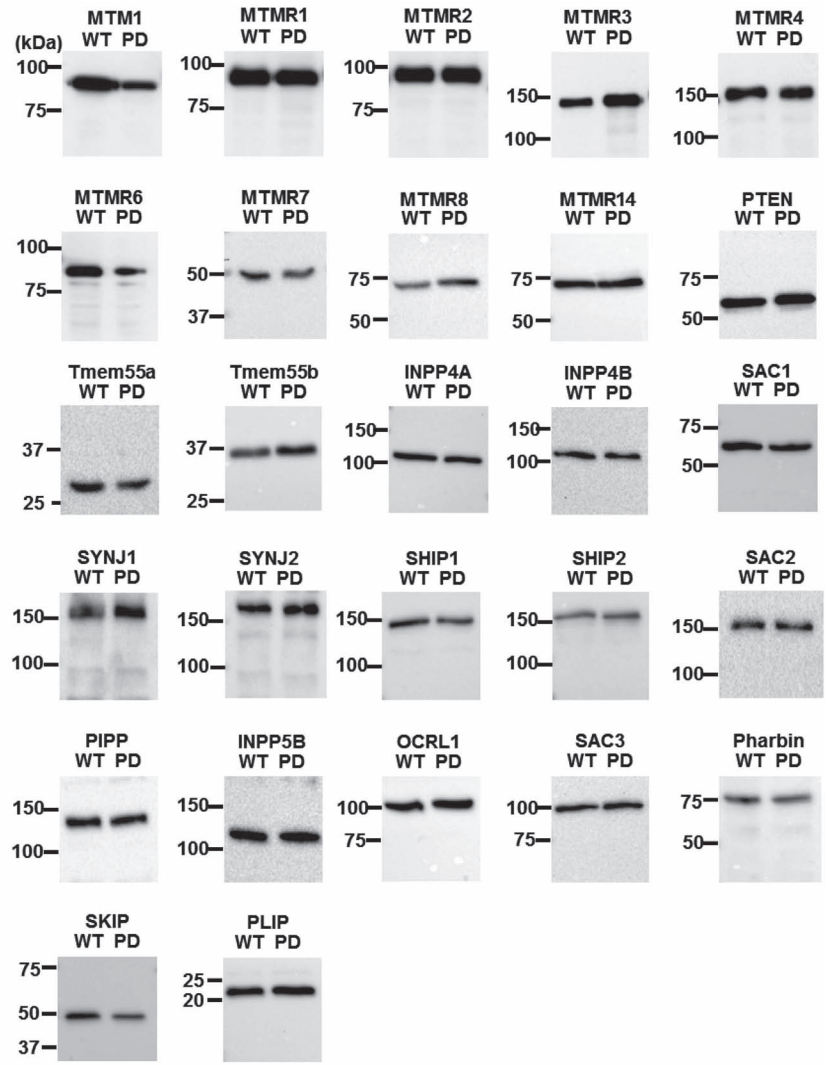

Fig. 1. Ectopic expression of phosphoinositide phosphatases.
HeLa cells were transfected with FLAG-tagged phosphoinositide phosphatase expression vectors. After 24 h, lysates of these cultures were subjected to Western blot analysis using an anti-FLAG antibody.

phosphoinositide phosphatases (WT and PD) were confirmed by Western blotting using lysates from HeLa cells transfected with the plasmids (Fig. 1). We then visualized the changes in cell morphology upon overexpression of the individual enzyme using a differential interference contrast (DIC) microscope. Interestingly, MTMR14-transfected HeLa cells displayed a drastically altered morphology with endocytic membrane vacuolation (Fig. 2 left panels). It should be noted that lucent vacuoles were observed only in the cells transfected with MTMR14 WT but not with other phosphoinositide phosphatases or the MTMR14 PD. The enlarged endosomes appeared to be lysosomes/late endosomes, as evidenced by the association of lysosome associated membrane protein 1 (LAMP1) to the limiting membranes (Fig. 2 right panels). Appearance of the LAMP1-positive swollen endosomes in the MTMR14 transfected cells is reminiscent of the vacuoles observed in the PIPKIII-deficient

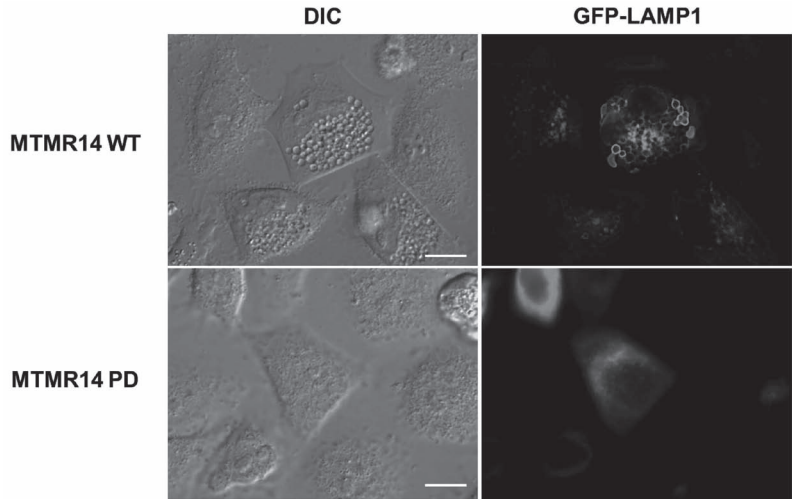

Fig. 2. Vacuolation of HeLa cells overexpressing MTMR14 WT, but not PD.
Cells were transfected with expression vectors either for MTMR14 WT or PD together with a GFP-LAMP1 expression plasmid. DIC and fluorescent images were captured after 24 h. Scale bar : 10 μm.

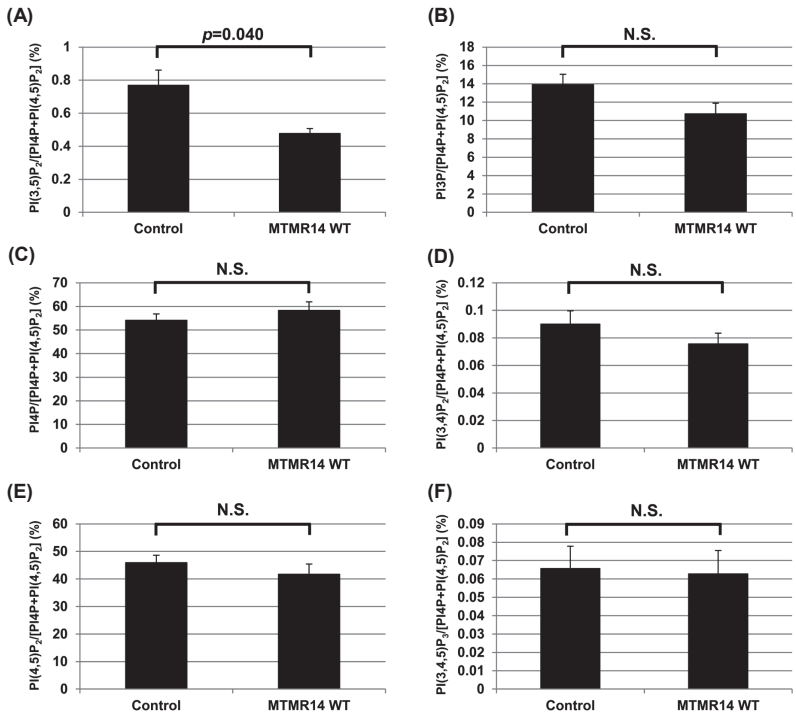

Fig. 3. Reduction of cellular $PI(3,5)P_2$ by overexpression of MTMR14.
HeLa cells were labeled with [^{32}P]orthophosphate under steady-state conditions. Lipids were extracted from MTMR14 WT or PD (Control) transfected HeLa cells, and the indicated phosphoinositides were analyzed by HPLC. Levels of $PI(3,5)P_2$ (A), PI3P (B), PI4P (C), $PI(3,4)P_2$ (D), $PI(4,5)P_2$ (E), and $PI(3,4,5)P_3$ (F) are expressed as a percentage of the levels of PI4P plus $PI(4,5)P_2$ (mean±SEM ; $n=3$). N.S. indicates $p>0.05$.

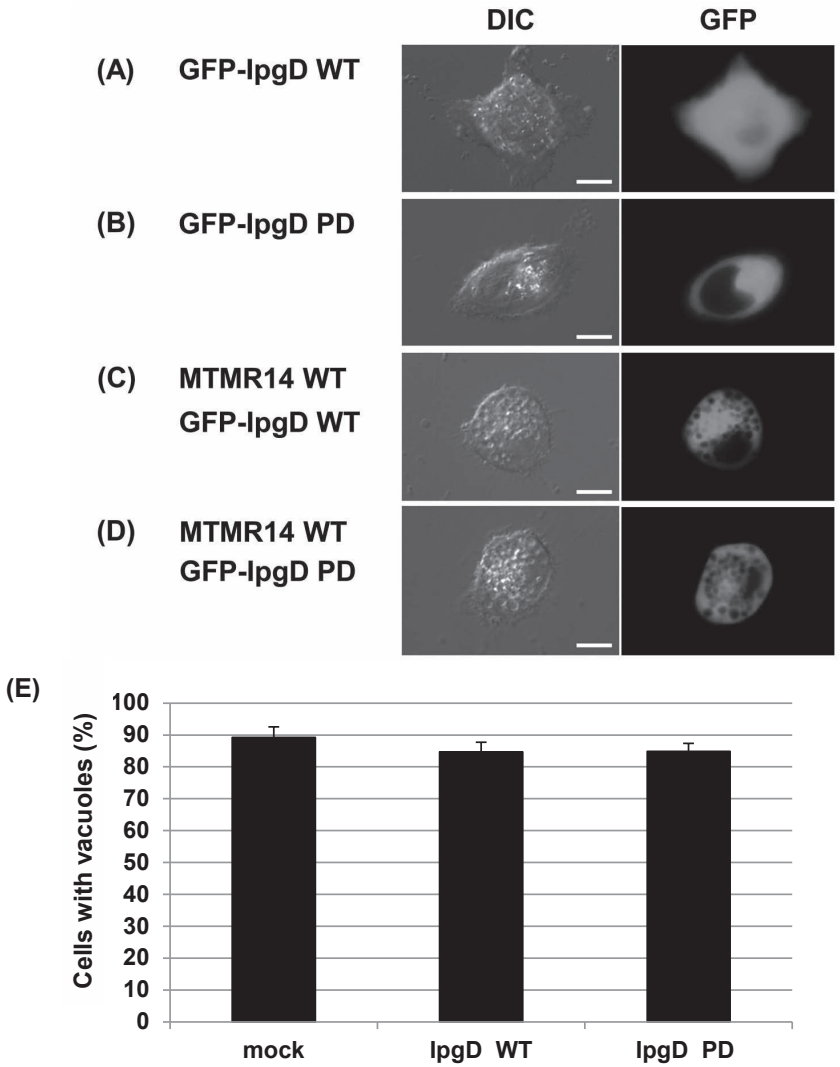

Fig. 4. Effects of the PI5P-producing enzyme on vacuolation.
A-D, GFP-IpgD WT (A, C) or PD (B, D) were expressed in HeLa cells alone (A, B) or together with MTMR14 WT (C, D). Representative data of each condition are shown. Scale bar : 10 μm. E, HeLa cells expressing IpgD WT or PD were treated for 4 h with 2.5 μM YM201636. The percentage of cells with vacuoles in each condition is shown (mean±SEM ; n=3).

murine embryonic stem (ES) cells, fibroblasts and intestinal epithelial cells[8].

We have reported that PI(3,5)P_2 levels were reduced while PI3P (the substrate of PIPKIII) levels were increased in PIPKIII-deficient ES cells[8], suggesting that the decrease in PI(3,5)P_2 and/or the accumulation of PI3P may underlie the formation of swollen lysosomes in the PIPKIII$^{-/-}$ cells. MTMR14 is reported to dephosphorylate PI3P and PI(3,5)P_2 *in vitro*[15]. We wondered if PI3P and PI(3,5)P_2 levels could be reduced in the MTMR14 transfected cells, which might be involved in the formation of swollen lysosomes in the cells. To test this, we examined the levels of phosphoinositides in HeLa cells by HPLC analysis. In ^{32}Pi-labeled cells, MTMR14 over-

expression showed the percentage of PI(3,5)P_2 in PI4P plus PI(4,5)P_2 in its phosphatase activity dependent manner (Fig. 3). There was no significant difference in the levels of PI4P, PI(3,4)P_2, PI(4,5)P_2, or PI(3,4,5)P_3 among MTMR14- and phosphatase-inactive MTMR14-transfected cells. PI5P was below the detection limit of our HPLC analyses. Our data indicate that PI(3,5)P_2 levels were reduced in the MTMR14-transfected cells with swollen lysosomes. PI(3,5)P_2 depletion but not the concomitant increase in PI3P is the major contributing factor for the vacuolation phenotype in the PIPKIII-deficient cells[8]. In line with this notion, Dong, X.P. *et al*. reported that TRPML1, a PI(3,5)P_2 binding protein, restored vacuolation phenotype caused by a PI(3,5)P_2 depletion[16]. These results suggest that PI(3,5)P_2 is a critical phosphoinositide species which determines the size of lysosomes.

Relatively little is currently known about the physiological functions of PI5P. One would expect PI5P accumulation upon overexpression of MTMR14, since MTMR14 is a PI(3,5)P_2 3-phosphatase[15]. Conversely, it was previously shown that PI5P could be formed through phosphorylation of PI by PIPKIII, and thus inactivation of PIPKIII might lead to a reduction in cellular PI5P[8]. We then examined whether altered PI5P levels were implicated in the vacuolation of cells overexpressing MTMR14 or those lacking PIPKIII activity. To modulate cellular PI5P, we took advantage of a bacterial phosphatase IpgD, known to dephosphorylate PI(4,5)P_2 and produce PI5P[17]. HeLa cells were transfected with expression constructs coding either IpgD WT or PD. Neither of the IpgD constructs caused any changes in the morphology of lysosomes (Fig. 4A, B). Furthermore, vacuoles induced by MTMR14 WT expression were not affected by co-expressing IpgD (Fig. 4C, D). Consistent with previous reports[18], we detected enlarged lysosomes in HeLa cells treated with the potent PIPKIII inhibitor, YM201636. Overexpression of IpgD had no effect on the ability of the PIPKIII inhibitor to cause vacuolation, suggesting that depletion of PI5P does not underlie the formation of swollen lysosomes upon PIPKIII inactivation (Fig. 4E). Taken together, our results demonstrate that PI5P does not play a major role in the control of size and morphology of lysosomes.

In summary, our data implicates PI(3,5)P_2 as a regulator of lysosomal morphology and identifies MTMR14 as a potential enzyme metabolizing this lipid. MTMR14 is mutated in centronuclear myopathy, a severe childhood muscle disorder[15]. Mutations in PIPKIII have also been linked to fleck corneal dystrophy[19]. Thus, our findings may provide a new insight into how altered phosphoinositide metabolism may be linked to these human diseases and to malfunction of intracellular quality control. It will be of great interest to investigate whether the PIPKIII/PI(3,5)P_2/MTMR14 axis is involved in other disorders and how this specific phosphoinositide exerts its function in lysosomes in the future.

References

1) Filocamo, M. and Morrone, A. (2011) Lysosomal storage disorders : molecular basis and laboratory testing. *Hum. Genomics*, **5**, 156-169.
2) Lieberman, A.P., Puertollano, R., Raben, N., Slaugenhaupt, S., Walkley, S.U. and Ballabio, A. (2012) Autophagy in lysosomal storage disorders. *Autophagy*, **8**, 719-730.
3) Kollmann, K., Damme, M., Markmann, S., *et al*. (2012) Lysosomal dysfunction causes neurodegeneration in mucolipidosis II 'knock-in' mice. *Brain*, **135**, 2661-2675.
4) Tanaka, Y., Guhde, G., Suter, A., Eskelinen, E.L., Hartmann, D., Lullmann-Rauch, R., Janssen, P.M., Blanz, J., von Figura, K. and Saftig, P. (2000) Accumulation of autophagic vacuoles and cardiomyopathy in LAMP-2-deficient mice. *Nature*, **406**, 902-906.
5) Taddei, T.H., Kacena, K.A., Yang, M., Yang, R., Malhotra, A., Boxer, M., Aleck, K.A., Rennert, G., Pastores, G.M. and Mistry, P.K. (2009) The underrecognized progressive nature of N370S Gaucher disease and assessment of cancer risk in 403 patients. *Am. J. Hematol.*, **84**, 208-214.
6) Bonneick, S., Boentert, M., Berger, P., Atanasoski, S., Mantei, N., Wessig, C., Toyka, K.V., Young, P. and Suter, U. (2005) An animal model for Charcot-Marie-Tooth disease type 4B1. *Hum. Mol. Genet.*, **14**, 3685-3695.
7) Jaber, N., Dou, Z., Lin, R.Z., Zhang, J. and Zong, W.X. (2012) Mammalian PIK3C3/VPS34 : the key to

autophagic processing in liver and heart. *Autophagy*, **8**, 707–708.

8) Takasuga, S., Horie, Y., Sasaki, J., *et al.* (2013) Critical roles of type III phosphatidylinositol phosphate kinase in murine embryonic visceral endoderm and adult intestine. *Proc. Natl. Acad. Sci. U S A*, **110**, 1726–1731.

9) Sasaki, T., Takasuga, S., Sasaki, J., Kofuji, S., Eguchi, S., Yamazaki, M. and Suzuki, A. (2009) Mammalian phosphoinositide kinases and phosphatases. *Prog. Lipid. Res.*, **48**, 307–343.

10) Iizuka, R., Takasuga, S., Sato, Y., Asanuma, K., Sasaki, J. and Sasaki, T. (2008) Mammalian type III phosphatidylinositol phosphate kinase is dispensable for cell growth and survival. *Akita J. Med.*, **35**, 41–46.

11) Sbrissa, D., Ikonomov, O.C. and Shisheva, A. (1999) PIKfyve, a mammalian ortholog of yeast Fab1p lipid kinase, synthesizes 5-phosphoinositides. Effect of insulin. *J. Biol. Chem.*, **274**, 21589–21597.

12) Blondeau, F., Laporte, J., Bodin, S., Superti-Furga, G., Payrastre, B. and Mandel, J.L. (2000) Myotubularin, a phosphatase deficient in myotubular myopathy, acts on phosphatidylinositol 3-kinase and phosphatidylinositol 3-phosphate pathway. *Hum. Mol. Genet.*, **9**, 2223–2229.

13) Schaletzky, J., Dove, S.K., Short, B., Lorenzo, O., Clague, M.J. and Barr, F.A. (2003) Phosphatidylinositol-5-phosphate activation and conserved substrate specificity of the myotubularin phosphatidylinositol 3-phosphatases. *Curr. Biol.,* **13**, 504–509.

14) Walker, D.M., Urbe, S., Dove, S.K., Tenza, D., Raposo, G. and Clague, M.J. (2001) Characterization of MTMR3 : an inositol lipid 3-phosphatase with novel substrate specificity. *Curr. Biol.,* **11**, 1600–1605.

15) Tosch, V., Rohde, H.M., Tronchere, H., Zanoteli, E., Monroy, N., Kretz, C., Dondaine, N., Payrastre, B., Mandel, J.L. and Laporte, J. (2006) A novel PtdIns3P and PtdIns(3,5)P2 phosphatase with an inactivating variant in centronuclear myopathy. *Hum. Mol. Genet.*, **15**, 3098–3106.

16) Dong, X.P., Shen, D., Wang, X., Dawson, T., Li, X., Zhang, Q., Cheng, X., Zhang, Y., Weisman, L.S., Delling, M. and Xu, H. (2010) PI(3,5)P2 controls membrane trafficking by direct activation of mucolipin Ca(2+) release channels in the endolysosome. *Nat. Commun.*, **1**, 38.

17) Niebuhr, K., Giuriato, S., Pedron, T., Philpott, D.J., Gaits, F., Sable, J., Sheetz, M.P., Parsot, C., Sansonetti, P.J. and Payrastre, B. (2002) Conversion of PtdIns(4,5)P2 into PtdIns(5)P by the S.flexneri effector IpgD reorganizes host cell morphology. *EMBO J.*, **21**, 5069–5078.

18) Jefferies, H.B., Cooke, F.T., Jat, P., *et al*. (2008) A selective PIKfyve inhibitor blocks PtdIns(3,5)P2 production and disrupts endomembrane transport and retroviral budding. *EMBO Rep.*, **9**, 164–170.

19) Kawasaki, S., Yamasaki, K., Nakagawa, H., Shinomiya, K., Nakatsukasa, M., Nakai, Y. and Kinoshita, S. (2012) A novel mutation (p.Glu1389AspfsX16) of the phosphoinositide kinase, FYVE finger containing gene found in a Japanese patient with fleck corneal dystrophy. *Mol. Vis.*, **18**, 2954–2960.